Engineering Structures 351 (2026) 121939

Contents lists available at ScienceDirect

Engineering Structures

journal homepage: www.elsevier.com/locate/engstruct

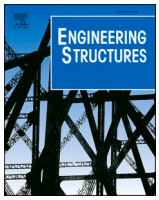

Out-of-plane stability design of stainless steel I-section beam-columns under moment gradients

Chunyan Quan [a,b,*], Fiona Walport [a,c], Merih Kucukler [b], Leroy Gardner [c]

[a] Department of Civil Environmental and Geomatic Engineering, University College London, London WC1E 6AE, UK
[b] School of Engineering, University of Warwick, Coventry CV4 7AL, UK
[c] Department of Civil and Environmental Engineering, South Kensington Campus, Imperial College London, London SW7 2AZ, UK

ARTICLE INFO

Keywords:
Beam-columns
Flexural-torsional buckling
I-sections
Moment gradients
Numerical modelling
Stainless steel

ABSTRACT

To address the limitations of existing design specifications for laterally unrestrained stainless steel I-section beam-columns, new design rules are proposed in this study. A comprehensive parametric study was conducted using finite element modelling to investigate the member behaviour and generate benchmark member resistances, covering Class 1–3 cross-sections and considering a range of material grades, member geometries and combined loading conditions. It was observed that the numerically derived compression-bending interaction factor for out-of-plane buckling checks decreases with more pronounced bending moment gradients, indicating their beneficial influence on member resistances. Thus, calibrated against the numerical results, a new formulation of the interaction factor is proposed, covering combined compression and uniform or non-uniform bending and ensuring alignment between member buckling and cross-section resistance checks. The new proposals are shown to provide accurate and consistent member resistance predictions for all load cases, and can be applied with the partial safety factor of 1.1 as specified in EN 1993–1–4:2025. These proposals have been included in the new version of the European structural stainless steel design standard EN 1993–1–4:2025.

1. Introduction

Stainless steel is being increasingly utilised in structural applications due to its favourable material properties, such as high corrosion resistance and ductility [1]. To date, extensive experimental and numerical research has been conducted into the behaviour and design of stainless steel cross-sections [2,3] and members [4,5]. At the member level, the buckling response of columns [6,7], beams [8–10] and beam-columns failing in-plane [11,12] have been studied, leading to the development of corresponding design rules. However, studies into the structural response of laterally unrestrained stainless steel beam-columns remain limited.

Current design rules [13,14] for laterally unrestrained stainless steel beam-columns take account of: (1) the cross-section type, with differentiation made between torsionally stiff members and torsionally flexible members, (2) the mode of buckling, with different formulae employed for in-plane (i.e. major axis) and out-of-plane (i.e. minor axis) instability, and (3) the presence of intermediate lateral restraints, with the calculations accounting for the segmental length between lateral restraints. The in-plane buckling design formulation adopted in EN 1993–1–4:2025 [15] was developed in [12] for austenitic stainless steel beam-columns and in [16] for duplex and ferritic stainless steel beam-columns. For the out-of-plane buckling check, following the methodology adopted in [17,18] for carbon steel I-section beam-columns, the EN 1993–1–4 design rules for austenitic stainless steel I-section beam-columns subjected to combined compression and uniform bending were developed in [19]. However, the design rules were not assessed for duplex and ferritic stainless steel members and are unsuitable for some non-uniform bending cases, e.g. when the ratio of bending moments applied at the two member ends ranges between −0.5 and −1. The aim of the present study is therefore to develop appropriate design rules for the out-of-plane buckling of laterally unrestrained stainless steel I-section beam-columns under combined compression and major axis uniform or non-uniform bending, covering all three main families of stainless steel – austenitic, duplex and ferritic – as well as a full range of moment gradients. The presented study includes extensive finite element (FE) analysis, accounting for various material grades, member geometries and loading conditions. Based on the generated FE

* Corresponding author at: Department of Civil Environmental and Geomatic Engineering, University College London, London WC1E 6AE, UK.
E-mail addresses: c.quan@ucl.ac.uk (C. Quan), f.walport@ucl.ac.uk (F. Walport), merih.kucukler@warwick.ac.uk (M. Kucukler), leroy.gardner@imperial.ac.uk (L. Gardner).

https://doi.org/10.1016/j.engstruct.2025.121939
Received 19 June 2025; Received in revised form 1 December 2025; Accepted 6 December 2025
Available online 2 January 2026

results, and employing a similar approach to that used in [17–19], design rules for the out-of-plane buckling of stainless steel I-section beam-columns are developed. The accuracy and safety of the new proposals are assessed, with a reliability analysis performed to verify the applicability of the new proposals in conjunction with a partial safety factor of 1.1, as specified in EN 1993–1–4:2025 [15].

2. EN 1993-1–4 design provisions for flexural-torsional buckling

In this section, the European provisions [13,15] for the flexural-torsional buckling design of stainless steel beam-columns provided in EN 1993–1–4:2025 are presented.

2.1. Compression

According to EN 1993–1–4:2025 [15], the design flexural buckling resistance of columns $N_{b,Rd}$ is calculated as:

$$N_{b,Rd} = \frac{\chi N_{Rk}}{\gamma_{M1}} \tag{1}$$

where N_{Rk} is the characteristic (unfactored) cross-sectional compression resistance, calculated as the product of the yield stress f_y and the full section area A for Class 1–3 cross-sections, and as the product of f_y and the effective section area A_{eff} for Class 4 cross-sections; γ_{M1} is the partial safety factor for instability checks of stainless steel members, taken as 1.1; and χ is the flexural buckling reduction factor, as given by:

$$\chi = \frac{1}{\phi + \sqrt{\phi^2 - \bar{\lambda}^2}} \leq 1.0 \tag{2}$$

$$\phi = 0.5\left[1 + \alpha(\bar{\lambda} - \bar{\lambda}_0) + \bar{\lambda}^2\right] \tag{3}$$

In Eqs. (2) and (3), α is the imperfection factor, equal to 0.49 and 0.76 for major and minor axis flexural buckling of stainless steel I-section members, respectively; $\bar{\lambda}_0$ is the limiting relative slenderness, equal to 0.2 for stainless steel I-section members; and $\bar{\lambda}$ is the relative member slenderness taken as:

$$\bar{\lambda} = \sqrt{N_{Rk}/N_{cr}} \tag{4}$$

where N_{cr} is the elastic flexural buckling load.

2.2. Major axis bending

According to EN 1993–1–4:2025 [15], the design lateral-torsional buckling (LTB) resistance of stainless steel I-section beams subjected to major axis bending $M_{b,Rd}$ is expressed through:

$$M_{b,Rd} = \chi_{LT}\frac{M_{Rk}}{\gamma_{M1}} \tag{5}$$

where M_{Rk} is the characteristic cross-sectional major axis bending moment resistance, calculated as the product of the yield stress f_y and the major axis section modulus W_y. For Class 1 and 2 cross-sections, W_y is taken as the plastic section modulus $W_{pl,y}$; for Class 3 cross-sections, W_y is taken as the elastic section modulus $W_{el,y}$; and for Class 4 cross-sections, W_y is taken as the effective section modulus $W_{eff,y}$.

For the design of carbon steel doubly-symmetric I-sections, a modified formulation for the calculation of the LTB reduction factor χ_{LT} was developed in [20] and has been included in EN 1993–1–1:2022 [13], as given by Eqs. (6)-(8),

$$\chi_{LT} = \frac{f_M}{\phi_{LT} + \sqrt{\phi_{LT}^2 - f_M\bar{\lambda}_{LT}^2}} \leq 1.0 \tag{6}$$

$$\phi_{LT} = 0.5\left[1 + f_M\left(\left(\frac{\bar{\lambda}_{LT}}{\bar{\lambda}_z}\right)^2\alpha_{LT}(\bar{\lambda}_z - 0.2) + \bar{\lambda}_{LT}^2\right)\right] \tag{7}$$

$$\bar{\lambda}_{LT} = \sqrt{M_{Rk}/M_{cr}} \tag{8}$$

where f_M is a factor that accounts for the influence of the shape of the bending moment distribution [21,22], $\bar{\lambda}_z$ is the normalised member slenderness for minor axis flexural buckling and M_{cr} is the elastic critical buckling bending moment. In EN 1993–1–1:2022 [13], the LTB imperfection factor α_{LT} is defined as a function of the major $W_{el,y}$ and minor $W_{el,z}$ axis elastic section moduli. Taking the same format as Eqs. (6)-(8) for carbon steel design, Fortan and Rossi [9,10] derived two sets of imperfection factor expressions α_{LT} for the LTB design of stainless steel members – see Table 1. The α_{LT} expressions, which are dependent on both the cross-sectional and material properties, have been included in EN 1993–1–4:2025 [15] and were adopted in the current study.

2.3. Combined compression and major axis bending

According to EN 1993–1–4:2025 [15], the stability of laterally unrestrained stainless steel I-section beam-columns subjected to combined compression and uniaxial major axis bending moment should be verified using the same rules as in EN 1993–1–1:2022 [13] for carbon steel design by satisfying the following expressions:

$$\frac{N_{Ed}}{N_{b,y,Rd}} + k_{yy}\frac{M_{y,Ed} + N_{Ed}e_{Ny}}{M_{b,y,Rd}} \leq 1.0 \tag{9}$$

$$\frac{N_{Ed}}{N_{b,z,Rd}} + k_{zy}\frac{M_{y,Ed} + N_{Ed}e_{Ny}}{M_{b,y,Rd}} \leq 1.0 \tag{10}$$

Eqs. (9) and (10) are used for the in-plane (major axis) and out-of-plane (minor axis) buckling checks, respectively. N_{Ed} and $M_{y,Ed}$ are the applied axial force and maximum major axis bending moment along the member length, respectively, while $N_{b,y,Rd}$ and $N_{b,z,Rd}$ are the design flexural buckling resistances about the major or minor axis of the member, respectively, as defined in Section 2.1. $M_{b,y,Rd}$ is the design LTB resistance of the member, as defined in Section 2.2, and e_{Ny} is the shift in the centroid axis for Class 4 cross-sections subjected to pure compression, which is equal to 0 for I-sections. For I-sections, the interaction factors k_{yy} developed for austenitic [12], duplex and ferritic [16] stainless steel have been incorporated in EN 1993–1–4:2025 [15], as presented in Table 2, where C_{my} is the equivalent uniform moment factor calculated on the basis of the ratio of end bending moments ψ:

$$C_{my} = 0.6 + 0.4\psi \geq 0.4 \tag{11}$$

The out-of-plane stability design of stainless steel beam-columns, requiring the definition of the interaction factor k_{zy}, is the focus of the present study. All grades of stainless steel and varying moment gradients are addressed.

In addition to in-plane and out-of-plane member stability checks (i.e. Eqs. (9) and (10)), the cross-section resistance of beam-columns must also be verified. According to EN 1993–1–4:2025 [15], designers are directed to use the carbon steel design rules in EN 1993–1–1:2022 [13] for the cross-section resistance check of stainless steel cross-sections under combined compression and bending. The compression-reduced design cross-section major axis bending resistance $M_{N,y,Rd}$ for Class 1

Table 1
Imperfection factor α_{LT} for lateral-torsional buckling of stainless steel doubly symmetric I- and H-sections [15].

Stainless steel grade	α_{LT}
Austenitic	$0.31\sqrt{W_{el,y}/W_{el,z}} \leq 1.10$
Duplex	$0.23\sqrt{W_{el,y}/W_{el,z}} \leq 0.76$
Ferritic	$0.27\sqrt{W_{el,y}/W_{el,z}} \leq 0.76$

Table 2
Interaction factor k_{yy} for in-plane (major axis) buckling check of stainless steel doubly symmetric I-sections.

Austenitic	Duplex	Ferritic
For $\bar{\lambda}_y < 1.0$:	For $\bar{\lambda}_y < 1.3$:	For $\bar{\lambda}_y < 1.3$:
$C_{my}[1 + 2.50(\bar{\lambda}_y - 0.35)n_y]$	$C_{my}[1 + 2.00(\bar{\lambda}_y - 0.30)n_y]$	$C_{my}[1 + 1.60(\bar{\lambda}_y - 0.35)n_y]$
For $\bar{\lambda}_y \geq 1.0$:	For $\bar{\lambda}_y \geq 1.3$:	For $\bar{\lambda}_y \geq 1.3$:
$C_{my}(1 + 1.625n_y)$	$C_{my}(1 + 2.00n_y)$	$C_{my}(1 + 1.52n_y)$

and 2 I-sections is given by:

$$M_{N,y,Rd} = M_{pl,y,Rd}\frac{1-n}{1-0.5a} \leq M_{pl,y,Rd} \tag{12}$$

where n is equal to the ratio of the applied axial force to the plastic compression resistance, i.e. $N_{Ed}/N_{pl,Rd}$, and a is equal to $(A\text{-}2bt_f)/A$ but no greater than 0.5; b and t_f are the flange width and thickness, respectively.

For Class 3 and 4 I-sections, a linear interaction relationship between cross-sectional compression N_{Rd} and major axis bending resistance $M_{y,Rd}$ is used as given by:

$$\frac{N_{Ed}}{N_{Rd}} + \frac{M_{y,Ed}}{M_{y,Rd}} \leq 1.0 \tag{13}$$

The ultimate member resistances are governed by the critical result from the in-plane and out-of-plane stability checks, along with the cross-section resistance check. Note that the pure compression and bending resistances used in these checks for beam-columns are determined according to the cross-section classification of members under combined compression and bending.

3. Finite element modelling

3.1. General

A finite element (FE) modelling study into the flexural-torsional buckling behaviour of laterally unrestrained stainless steel I-section beam-columns under moment gradients is presented in this section. The geometrically and materially nonlinear analyses with imperfections (GMNIA) were conducted using the FE analysis software Abaqus [23]. The four-noded general purpose shell finite element S4R, which accounts for transverse shear deformations and finite membrane strains with reduced integration and a large-strain formulation, as successfully employed in similar previous studies [24–27], was adopted. Each web and flange plate of the I-sections was subdivided into 16 elements, while the number of elements along the member length was chosen to

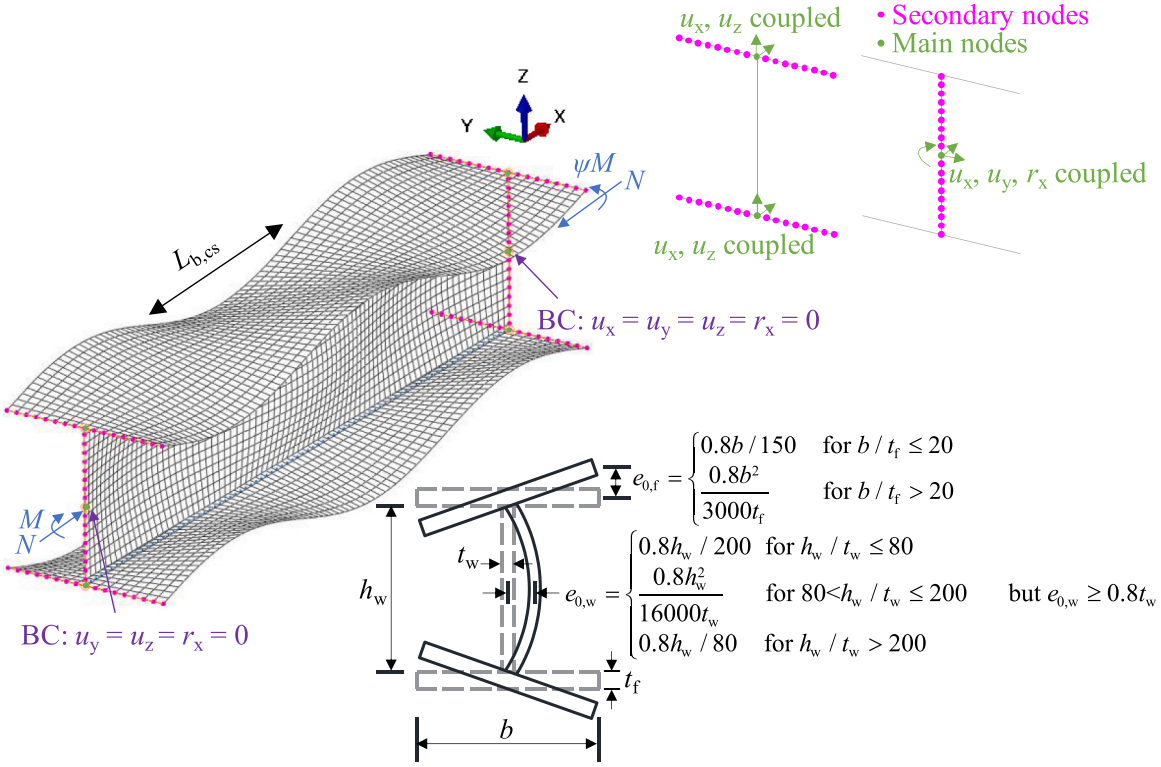

Fig. 1. Details of developed FE models.

Table 3
Adopted stainless steel material parameters for the FE models [33].

Grade	Young's modulus E (N/mm^2)	Yield (0.2% proof) stress f_y (N/mm^2)	Ultimate stress f_u (N/mm^2)	Ultimate strain ε_u	Strain hardening exponent n	Strain hardening exponent m
A	200000	280	580	0.50	9.1	2.3
D	200000	530	770	0.30	9.3	3.6
F	200000	320	480	0.16	17.2	2.8

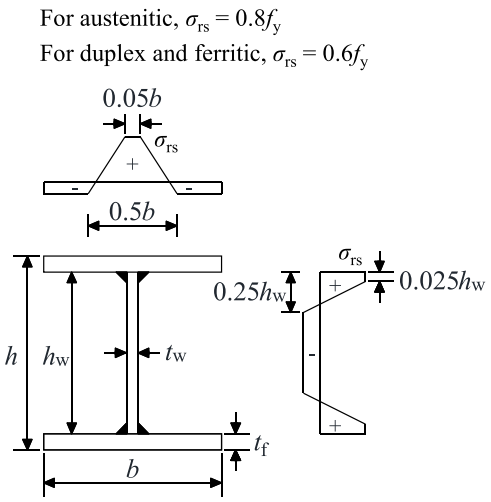

Fig. 2. Residual stress pattern adopted for welded stainless steel I-sections [40] (+ve = tension; -ve = compression).

maintain an element aspect ratio close to unity. The Simpson integration method was adopted, and five integration points were employed through the shell element thickness.

To avoid overlapping of the web and flange plates, the top and bottom web nodes were offset by half the flange thickness, in line with the approach adopted in [28,29], and the plates were connected by beam multi-point constraints. Fork-end support conditions enabling warping deformations but preventing twist were applied at the member ends by the application of kinematic coupling constraints. As illustrated in Fig. 1, the displacements u_x and u_z of all flange nodes were coupled to the flange centre, while the displacements u_x, u_y and rotation r_x of all web nodes including the web-flange junction (i.e. the flange centre) were coupled to the web centre. In line with the approach adopted in [30,31], these coupling constraints allow expansion in the flange and web plates while constraining the element nodes along the flange and web plates to remain in a straight line in the specified directions, thereby allowing free warping at the two end cross-sections. The boundary conditions (BC) were set with $u_y = u_z = r_x = 0$ at the web centre of one end and $u_x = u_y = u_z = r_x = 0$ at the web centre of the other end; this boundary condition configuration achieved the desired fork-end constraints while preventing twisting at both ends. Axial compression N and bending moments were applied simultaneously at the web centre of each end cross-section, with a bending moment M at one end and ψM at the other end, where ψ represents the bending moment ratio.

3.2. Material modelling

The two-stage Ramberg-Osgood (R-O) material model [32] was employed to represent the engineering stress-strain response of stainless steel, as given by Eqs. (14) and (15), where E is the Young's modulus, f_y is the yield stress, taken as 0.2% proof stress, $\varepsilon_{0.2}$ is the total strain at the

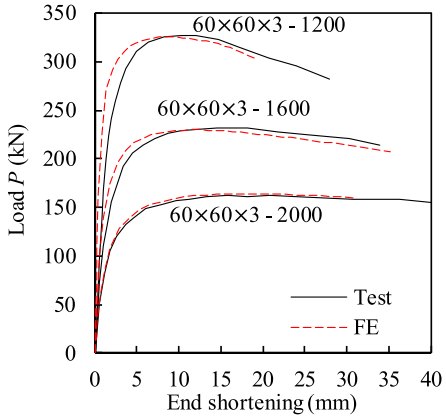

(a) Results in [44] validated against column tests in [45]

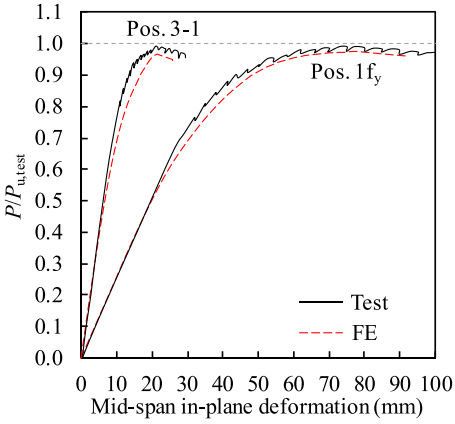

(b) Results in [29] validated against beam tests in [46]

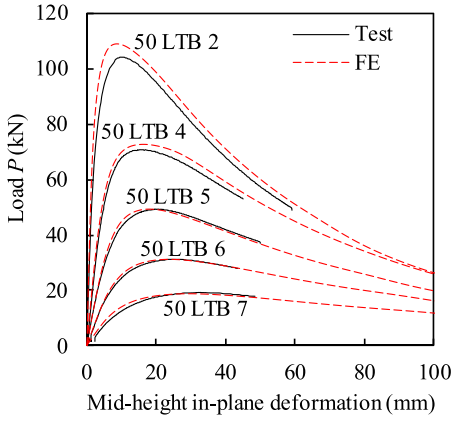

(c) Results in [19] validated against beam-column tests in [19]

Fig. 3. Load-deformation curves for validation of adopted FE modelling approach.

Table 4
Section profiles adopted for parametric study.

Grade	Austenitic			Duplex			Ferritic		
HEB	100	160	200	100	160	200	100	160	200
IPE	100	160	200	80	100	120	100	160	180
HEA	100	160	200	100	120	-	100	160	200
HEM	-	-	-	100	-	-	-	-	-
Custom ($h\times b\times t_f\times t_w$)	300 × 100 × 15 × 12			300 × 100 × 15 × 12			300 × 100 × 15 × 12		

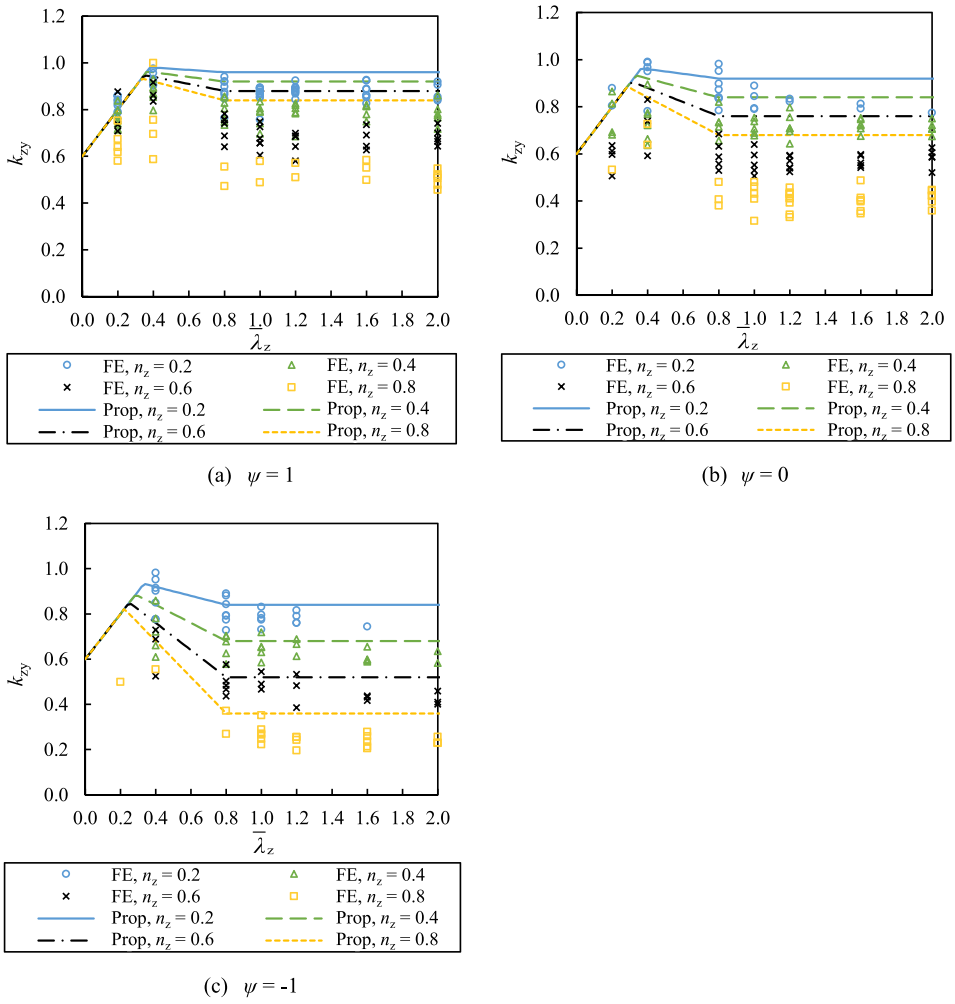

Fig. 4. Derivation of the proposed interaction factor $k_{zy,prop}$ (lines) based on the numerical values $k_{zy,FE}$ (points) for austenitic stainless steel beam-columns.

yield stress f_y, equal to 0.002 $+f_y/E$, E_y is the tangent modulus at the 0.2% proof stress, as given by Eq. (16), and n and m are the strain hardening exponents.

$$\varepsilon = \frac{\sigma}{E} + 0.002\left(\frac{\sigma}{f_y}\right)^n \text{ for } \sigma \le f_y \tag{14}$$

$$\varepsilon = \varepsilon_{0.2} + \frac{\sigma - f_y}{E_y} + \left(\varepsilon_u - \varepsilon_{0.2} - \frac{f_u - f_y}{E_y}\right)\left(\frac{\sigma - f_y}{f_u - f_y}\right)^m \text{ for } f_y < \sigma \le f_u \tag{15}$$

$$E_y = \frac{E}{1 + 0.002n\frac{E}{f_y}} \tag{16}$$

The standardised material properties provided in [33] for the three main families of stainless steel – austenitic (A), duplex (D) and ferritic (F) – were adopted herein, as summarised in Table 3. The engineering stress-strain curves were transformed to true stress-plastic strain relationships for input into Abaqus [23], with a Poisson's ratio of $\nu = 0.3$ in the elastic range and $\nu = 0.5$ in the plastic range.

3.3. Geometric imperfections and residual stresses

Given the important influence of imperfections on member stability [34], global and local geometric imperfections, as well as material imperfections (i.e. residual stresses) were incorporated into the shell FE models. The global geometric imperfection was applied in the form of the critical global buckling mode determined through a linear bifurcation analysis (LBA) under the applied loading, with an amplitude of 1/1000 of the member length L, i.e. L/1000. As shown in Fig. 1, the local geometric imperfections were applied to the shell FE models by adopting a series of sinusoidal subpanel imperfections with the wavelength defined equal to the elastic local buckling half-wavelength $L_{b,cs}$, which can be calculated using the expressions provided in [35]. The local geometric imperfection amplitudes were taken as 80% of the

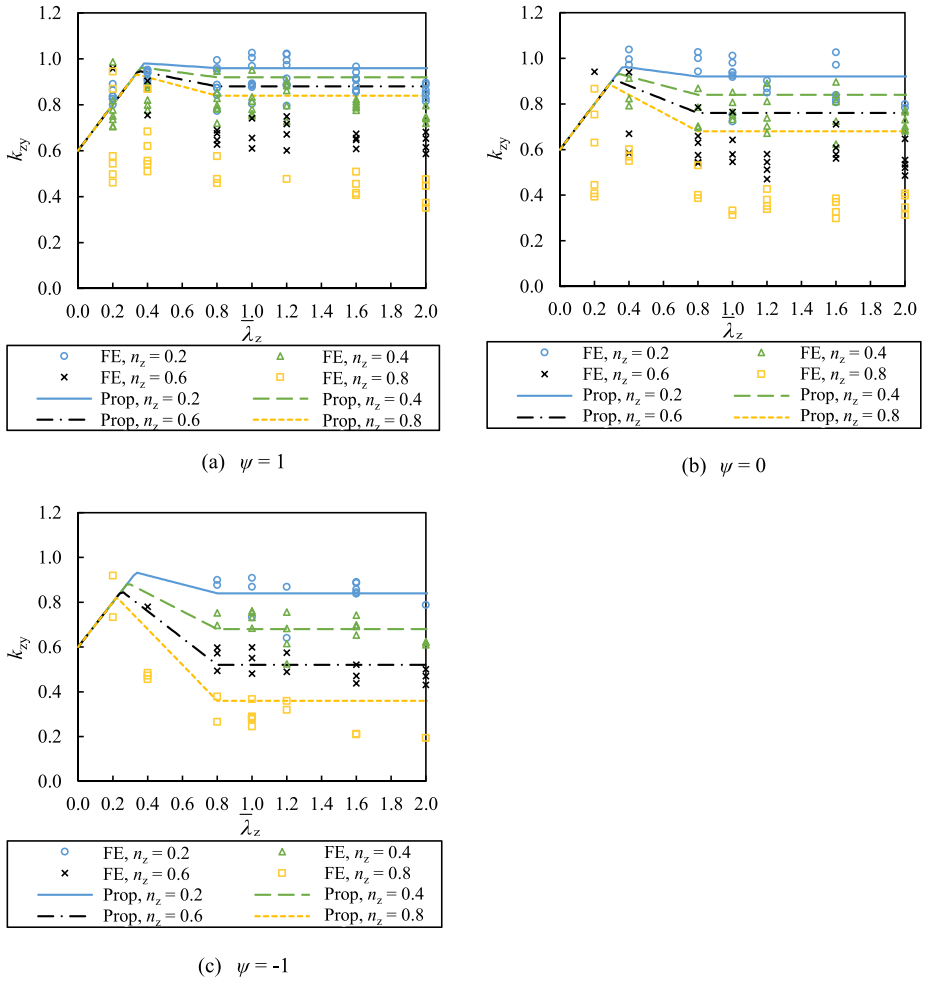

Fig. 5. Derivation of the proposed interaction factor $k_{zy,prop}$ (lines) based on the numerical values $k_{zy,FE}$ (points) for duplex stainless steel beam-columns.

manufacturing tolerance values provided in EN 1090–2 [36], as presented in Fig. 1, in line with the recommendations in EN 1993–1–5:2024 [37] and the new Eurocode for design by finite element analysis EN 1993–1–14:2025 [38], as well as relevant studies [31,39]. The tolerance values considered herein for the local geometric imperfections of the web and flange plates were taken as the smallest relevant tolerance value that must be met. This corresponds to criterion 7 (essential tolerance) of Table B1 for the web (i.e. the strictest tolerance of criteria 7–9 of Table B1) and criterion 2 (essential tolerance) of Table B3 for the flange (i.e. the strictest tolerance of criteria 1–2 of Table B3 and criteria 4–5 of Table B1) provided in EN 1090–2 [36]. For the cases where the web plates were more susceptible to local buckling than the flange plates, i.e. when the elastic local buckling stress of the isolated web plate with simply-supported boundary conditions $\sigma_{cr,w}$ was lower than that of the isolated flange plate $\sigma_{cr,f}$, the amplitude of the local web imperfection was taken as the $e_{0,w}$ value shown in Fig. 1. Similarly, for the cases where the flange plates were more susceptible to local buckling than the web plate, the amplitudes of the local flange imperfections were taken as the $e_{0,f}$ value shown in Fig. 1. The local imperfection amplitudes of the non-critical plate elements were defined such that the web-to-flange junctions remained at 90°. In the calculation of $e_{0,w}$ and $e_{0,f}$, h_w and t_w are the web height and thickness, respectively, and b and t_f are the flange width and thickness, respectively. Residual stresses were explicitly defined based on the stainless steel welded I-section residual stress distribution proposed by Yuan et al. [40], as shown in Fig. 2, by introducing an initial stress condition with corresponding plastic strains [41].

3.4. Validation and parametric study

The developed FE modelling approach has been successfully utilised in relevant studies by other researchers [30,42,43] and also employed and validated in the present authors' previous studies: in [44], models were validated against the results of stainless steel column tests [45]; in [29], models were validated against the results of carbon steel beam tests [46]; and in [19], models were validated against the results of stainless steel beam-column tests [19]. The developed FE modelling approach has been found to successfully capture the buckling behaviour and failure modes of structural steel and stainless steel members, with numerical ultimate member resistances closely matching the experimental results. Additionally, the numerical load-deformation curves align well with those observed in the experiments, as shown in Fig. 3, where P is the applied load and $P_{u,test}$ is the ultimate load obtained from the tests. More details of the FE model validation can be found in [19,29,44]. The previous validated FE modelling approach was therefore employed for generating the benchmark data herein.

For the parametric study, a total of 3250 beam-columns were evaluated covering a range of stainless steel material grades, cross-section geometries, member lengths and loading conditions. The stainless steel material properties employed in the parametric studies are provided in Table 3. For each material grade, ten I-sections covering Class 1–3 were considered, as listed in Table 4, including nine standard European I-section profiles with height-to-width ratios h/b ranging from 0.95 to 2 and one custom I-section with $h/b = 3$. Beam-columns with seven different lengths were modelled for each considered cross-section,

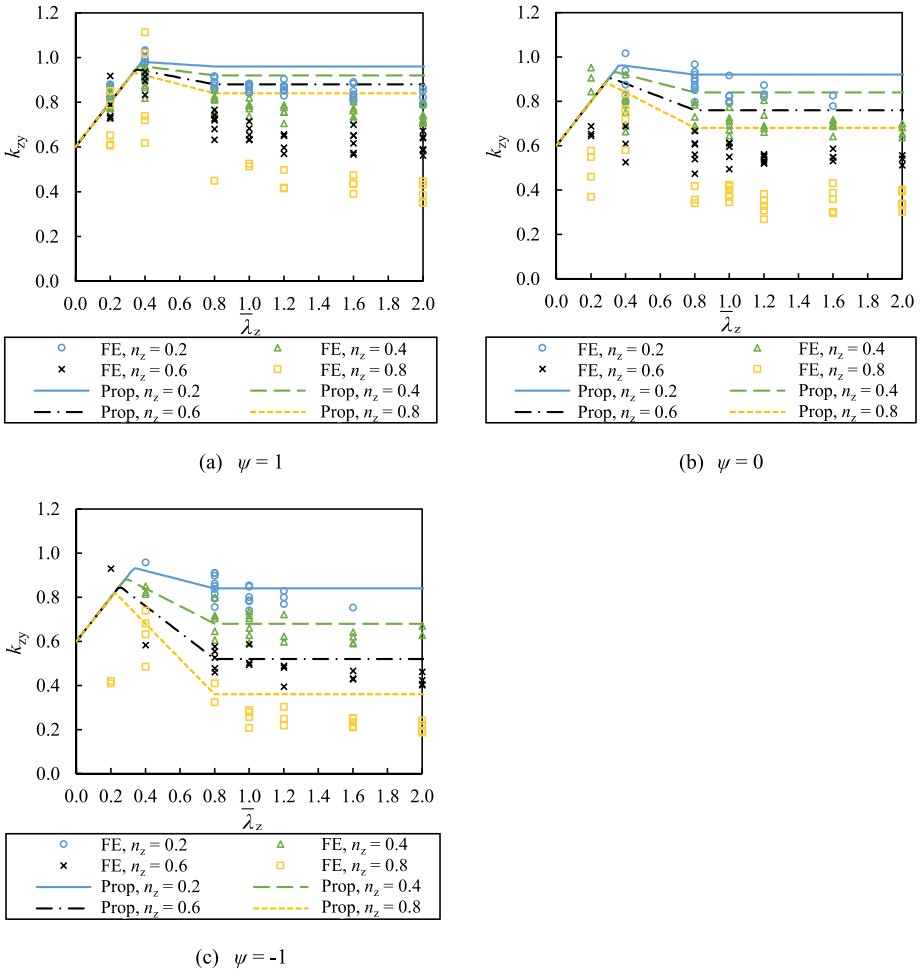

Fig. 6. Derivation of the proposed interaction factor $k_{zy,prop}$ (lines) based on the numerical values $k_{zy,FE}$ (points) for ferritic stainless steel beam-columns.

with the member lengths L selected such that the member relative flexural buckling slenderness values about the minor axis $\bar{\lambda}_z$ were equal to 0.2, 0.4, 0.8, 1.0, 1.2, 1.6 and 2.0. A range of major axis bending-to-axial compressive load ratios M/N was defined, equivalent to applying ten initial loading eccentricities e_n = 10, 20, 50, 80, 120, 160, 240, 320, 460 and 600 mm. Additionally, three bending moment distributions along the member length were investigated by changing the ratio of the applied end bending moments $\psi = 1$, 0 and −1. As illustrated in Fig. 1, the beam-columns were subjected to an axial force N, along with bending moments $M = Ne_n$ applied at one member end and $\psi M = \psi Ne_n$ applied at the other member end. For each design case, the ultimate axial load N_{FE} and maximum major axis bending moment along the member length M_{FE} were obtained from the results of the GMNIA.

4. Development of interaction factor k_{zy}

Based on the numerical results from the parametric study, proposals are made in this section for determining the interaction factor k_{zy} for beam-columns made of various stainless steel grades under combined compression and uniform/non-uniform bending moments. The accuracy and safety of the proposals are evaluated, and a reliability analysis is conducted to verify the suitability of the proposals in conjunction with the partial safety factor $\gamma_{M1} = 1.1$, as recommended in EN 1993–1–4:2025 [15].

4.1. Calibration of interaction factors

The calibration of the interaction factor k_{zy} is presented in this section. This calibration was carried out against the numerically derived interaction factors $k_{zy,FE}$ based on the results of the parametric study provided in Section 3.4. In line with the format of Eq. (10) for the out-of-plane buckling check, the following expression for the interaction between the flexural buckling resistance and LTB resistance can be obtained:

$$\frac{N_{FE}}{N_{b,z,Rd}} + k_{zy,FE}\frac{M_{FE}}{M_{b,y,Rd}} = 1.0 \tag{17}$$

where $N_{b,z,Rd}$ and $M_{b,y,Rd}$ are the minor axis flexural buckling resistance and LTB resistance determined from Eqs. (1) and (5), respectively. Note that the partial safety factor 1.1 was not incorporated in the determination of $N_{b,z,Rd}$ and $M_{b,y,Rd}$, such that the characteristic resistance values were obtained. The calculation of the LTB resistance $M_{b,y,Rd}$ aligns with the provisions in EN 1993–1–4:2025 [15] (which differ from those in EN 1993–1–4:2006 [14]). Rearranging Eq. (17), the numerically derived interaction factor $k_{zy,FE}$ can be expressed as:

$$k_{zy,FE} = \left(1 - \frac{N_{FE}}{N_{b,z,Rd}}\right)\frac{M_{b,y,Rd}}{M_{FE}} \tag{18}$$

The numerically derived interaction factors $k_{zy,FE}$ for the austenitic, duplex and ferritic stainless steel beam-columns are presented in Figs. 4–6, respectively. The results have been grouped based on the ratio of the applied end bending moments ψ, as well as the ratio of the applied axial force to the minor axis flexural buckling resistance $n_z = N_{FE}/N_{b,z,Rd}$.

Following the same approach as employed in [17,18] for carbon steel

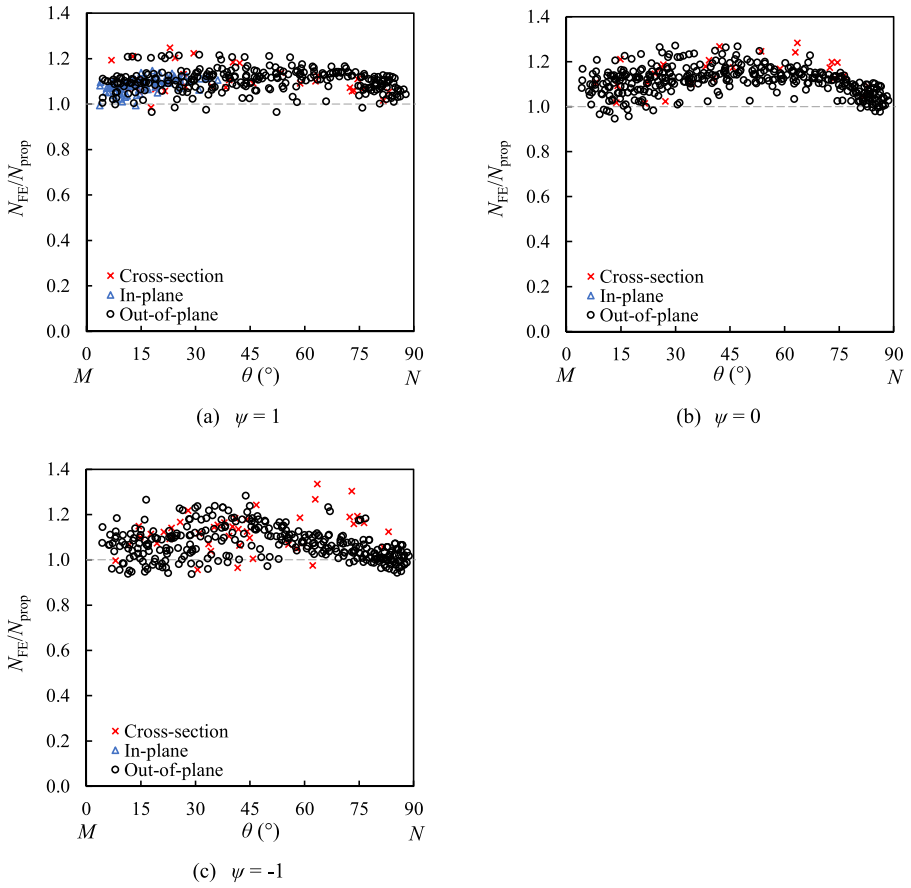

Fig. 7. Comparison of ultimate axial load predicted by the proposed design rules N_{prop} against shell FE results N_{FE} for austenitic stainless steel beam-columns, indicating the critical design check.

design and calibrated against $k_{zy,FE}$, the proposed interaction factor $k_{zy,prop}$ for stainless steel design is:

$$k_{zy,prop} = \begin{cases} 1 - \dfrac{0.2\bar{\lambda}_z n_z}{C_{mLT} - 0.2} & \text{for } \bar{\lambda}_z < 0.8 \\ 1 - \dfrac{0.16 n_z}{C_{mLT} - 0.2} & \text{for } \bar{\lambda}_z \geq 0.8 \end{cases} \tag{19}$$

$$\text{but } k_{zy,prop} \leq 0.6 + \bar{\lambda}_z \quad \text{for } \bar{\lambda}_z < 0.4 \tag{20}$$

where the equivalent uniform moment factor for LTB C_{mLT} is determined from:

$$C_{mLT} = 0.6 + 0.4\psi \geq 0.4 \tag{21}$$

Note that Eq. (19) alone gives a proposed interaction factor $k_{zy,prop}$ defined in a bi-linear format. For $\bar{\lambda}_z \geq 0.8$, $k_{zy,prop}$ remains constant, mirroring the behaviour observed from the numerical values $k_{zy,FE}$, which tend to remain approximately constant within this slenderness range, while for $\bar{\lambda}_z$ values decreasing from 0.8 to 0, $k_{zy,prop}$ increases towards 1.0. However, this simplified bi-linear form of k_{zy} does not fully capture the observed behaviour, where a reduction in the numerical interaction factor values $k_{zy,FE}$ is seen for $\bar{\lambda}_z < 0.4$. Therefore, an additional limit is introduced, as expressed by Eq. (20), whereby the factor $k_{zy,prop}$ decreases to 0.6 as $\bar{\lambda}_z$ approaches 0. This mirrors the formulae developed in [17,18] for carbon steel design and included in EN 1993–1–1:2022 [13], which enables the full exploitation of the convex plastic compression-bending cross-section resistance for stocky members with $\bar{\lambda}_z \leq 0.4$. Given the rounded stress-strain response of stainless steel, which results in plasticity being experienced by all cross-sections in the Class 1–3 range, a single set of formulae, Eqs. (19) and (20), is proposed for all non-slender cross-sections in this study. This approach is consistent with the provisions of EN 1993–1–4:2025 [15], in which the same formulae are used for all classes of stainless steel cross-sections, as well as EN 1993–1–1:2022 [13] for carbon steel, where the same formulae are applied to Class 1 and 2 cross-sections, and Class 3 (semi-compact) cross-sections when the elastic-plastic moment resistance is employed.

As shown in Figs. 4–6, the numerically derived interaction factor values $k_{zy,FE}$ decrease for beam-columns as the bending moment distribution changes from uniform ($\psi = 1$) to antisymmetric ($\psi = -1$), indicating the beneficial effects of bending moment gradients on member resistances. This is mirrored in the proposed interaction factor $k_{zy,prop}$, which also decreases with increasing moment gradient levels through the equivalent uniform moment factor for LTB C_{mLT}, as expressed in Eq. (21), which effectively captures this beneficial effect. It should be noted that the beneficial effect from moment gradients on member resistances is also partially accounted for in the determination of the LTB reduction factor χ_{LT}. Thus, the effect captured in the compression-bending interaction factor k_{zy} was adjusted accordingly.

It can be seen from Figs. 4–6 that the majority of $k_{zy,FE}$ values are located below $k_{zy,prop}$, indicating that the proposed design approach generally provides safe-sided predictions of member resistances. Although the proposed $k_{zy,prop}$ shows less good agreement with $k_{zy,FE}$ at larger $n_z = N_{FE}/N_{b,z,Rd}$ values, it should be noted from the out-of-plane buckling check given by Eq. (10) that the interaction factor k_{zy} has less influence in compression-governed cases (i.e., at higher n_z values) and becomes more significant in bending-governed cases (i.e., at lower n_z values). Therefore, greater emphasis was placed on achieving good agreement with $k_{zy,FE}$ for smaller n_z values, where k_{zy} has a stronger effect. A similar trend was also reported in [17] for the out-of-plane

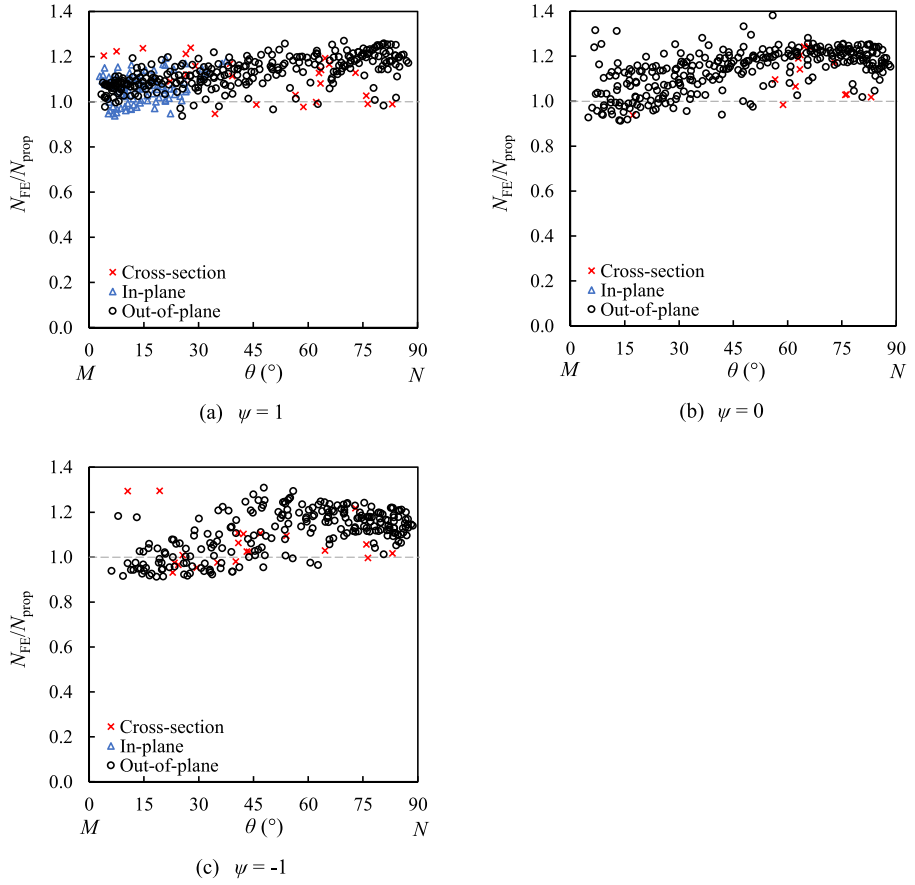

Fig. 8. Comparison of ultimate axial load predicted by the proposed design rules N_{prop} against shell FE results N_{FE} for duplex stainless steel beam-columns, indicating the critical design check.

stability design of steel beam-columns, which has been incorporated into EN 1993–1–1:2022 [13], and in [16] for the in-plane stability design of stainless steel beam-columns, which has been included in EN 1993–1–4:2025 [15]. Note that, according to EN 1993–1–4:2025 [15], in addition to the out-of-plane buckling check using the proposed interaction factor k_{zy}, the verification of the in-plane member stability and cross-section resistance, as introduced in Section 2.3, is also required. The critical result among these three checks determines the ultimate resistance of the beam-column.

4.2. Assessment of proposed design rules

The accuracy of the proposals is assessed against the benchmark shell FE results in this section. Figs. 7, 8 and 9 present the ratios of the ultimate axial loads obtained from the shell FE models N_{FE} to the predictions using the proposed design rules N_{prop} for the austenitic, duplex and ferritic stainless steel beam-columns, respectively. Note that although the ratios are presented in terms of the axial component of the loading, the combined influence of axial load and bending moment is duly considered. The radial angle θ [11] is employed to describe the relationship between the applied compression and bending, as determined below and illustrated in Fig. 10:

$$\theta = \tan^{-1}\left(\frac{N/N_{b,z,Rd}}{M/M_{b,y,Rd}}\right) \tag{22}$$

where M_{prop} is the predicted maximum major axis bending moment along the member length using the proposed design rules, and $\theta = 0°$ and $90°$ correspond to pure bending M and pure compression N, respectively.

As shown in Figs. 7–9, according to the proposed design rules, three dominant failure modes are observed for laterally unrestrained stainless steel beam-columns: cross-section failure, in-plane buckling and out-of-plane buckling. The majority of the studied beam-columns failed due to out-of-plane buckling, while some of the stockier members failed by cross-section failure. Additionally, there are some beam-columns under combined compression and uniform bending ($\psi = 1$) which exhibited in-plane buckling failure, particularly in bending dominating cases (i.e. low values of θ). Fig. 11 (a) and (b) illustrate the compression-bending interaction curves according to the proposed design rules for a stocky member with $\bar{\lambda}_z = 0.2$ and a slender member with $\bar{\lambda}_z = 1.6$, respectively. For the stocky member, the cross-section resistance generally governs, although in-plane buckling can be more critical in bending dominating scenarios. For the slender member, out-of-plane buckling is the dominant failure mode, with in-plane buckling becoming more critical in bending dominating cases.

Table 5 provides a summary of the mean, CoV, maximum and minimum values of the ratios of N_{FE}/N_{prop} for all studied members, where $N_{FE}/N_{prop} \geq 1$ indicates safe-sided predictions. The proposed design rules yield mean values of N_{FE}/N_{prop} close to 1.0 with low CoV values, indicating good consistency in the prediction of member resistances. The achieved accuracy and safety levels are comparable to those reported in previous studies [10,16] on stainless steel stability design. From Table 5 and Figs. 7–9, it can be seen that the ultimate resistances predicted using the proposed design rules are generally accurate and safe-sided compared against the benchmark shell FE results for the considered laterally unrestrained stainless steel beam-columns. The predictions are also consistent for both uniform and non-uniform bending cases.

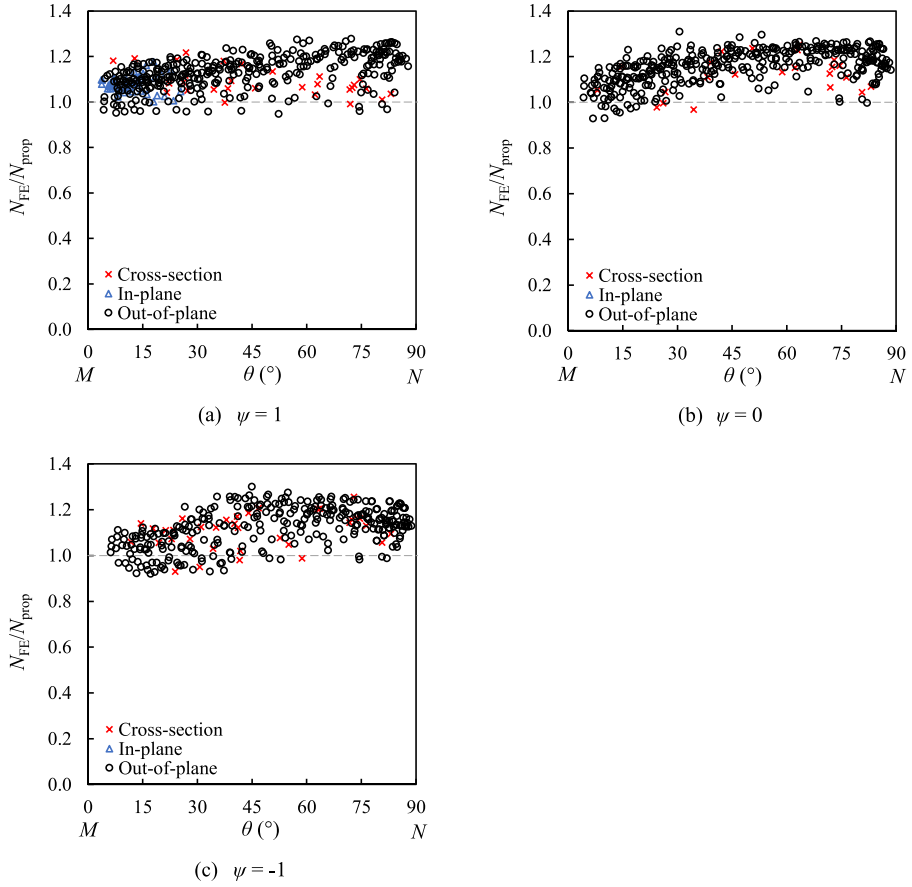

Fig. 9. Comparison of ultimate axial load predicted by the proposed design rules N_{prop} against shell FE results N_{FE} for ferritic stainless steel beam-columns, indicating the critical design check.

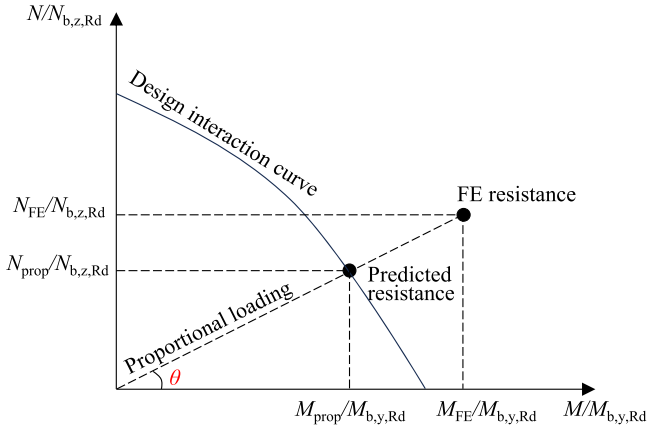

Fig. 10. Definition of radial angle θ for the combined compression and major axis bending loading condition.

4.3. Reliability analysis

The reliability analysis and required partial safety factors γ_{M1}* for use with the proposed design expressions are evaluated in this section. The first order reliability method (FORM), as set out in Annex D of EN 1990:2023 [47] and further detailed in [48], was employed to perform the reliability analysis. FORM provides an accurate and computationally efficient estimate of reliability [49,50]. This approach has been commonly adopted in the Eurocode background studies and in several independent investigations on buckling-related design expressions for steel and stainless steel members, such as [10,48,51,52].

Incorporating the dependency of the member resistance on the variability of the k basic variables, the coefficient of variation $V_{rt,i}$ was calculated for each considered case through:

$$V_{rt,i}^{\ 2} = \frac{1}{r_{t,i}(\underline{X}_m)^2} \sum_{j=1}^{k} \left(\frac{\partial r_{t,i}(X_j)}{\partial X_j} \sigma_j \right)^2 \tag{23}$$

where $r_{t,i}$ represents the theoretical resistance determined from the resistance model, $\underline{X}_m$ is an array containing the mean values of the basic variables and σ_j is the standard deviation of each basic variable j. For the design of stainless steel beam-columns, three basic variables were considered (i.e. $k = 3$): yield stress f_y, Young's modulus E and cross-sectional area A. With this assumption, Eq. (23) was simplified [53] to:

$$V_{rt,i} = \sqrt{\left(C_{1,i} V_{fy}\right)^2 + \left(C_{2,i} V_A\right)^2 + \left(C_{3,i} V_E\right)^2} \tag{24}$$

where $C_{1,i}$, $C_{2,i}$ and $C_{3,i}$ are the coefficients describing the dependency of the resistance model on the variables f_y, A and E for each modelled case i, calculated following the method in [54,55]. The adopted CoV values of the yield strength V_{fy} are listed in Table 6 as specified in [56], while the adopted CoV values of the cross-sectional area V_A were determined according to [53] and the CoV values of the Young's modulus V_E were taken as 0.03.

The mean correction factor b for the n considered cases, as listed in Table 6, was calculated based on the average ratio of the benchmark numerical resistance $r_{e,i}$ to the resistance predicted using the proposed design method with mean material properties $r_{t,i}$ for each case i, as expressed by [57,58]:

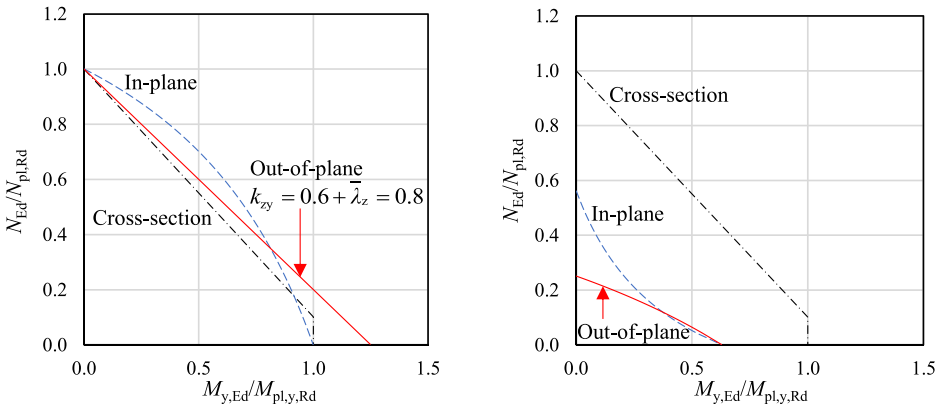

(a) Austenitic stainless steel beam-columns with HEB 200, $\bar{\lambda}_z = 0.2$, $\psi = 1$

(b) Austenitic stainless steel beam-columns with HEB 200, $\bar{\lambda}_z = 1.6$, $\psi = 1$

Fig. 11. Interaction curves of axial compression and major axis bending determined using the proposed design method for cross-section resistance, in-plane buckling and out-of-plane buckling checks.

Table 5
Summary of mean, CoV, maximum and minimum values of the ratios of N_{FE}/N_{prop} for all studied members.

Grade	Mean	CoV	Max.	Min.
Austenitic	1.10	0.059	1.34	0.94
Duplex	1.12	0.080	1.38	0.91
Ferritic	1.13	0.070	1.31	0.92

$$b = \frac{1}{n}\sum_{i=1}^{n}\frac{r_{e,i}}{r_{t,i}} \tag{25}$$

Finally, the mean required partial safety factor for the different considered cases was derived by:

$$\gamma_{M1}{}^{*} = \frac{1}{n}\sum_{i=1}^{n}\frac{r_{n,i}}{r_{d,i}} \tag{26}$$

where $r_{d,i}$ is the design resistance determined as a function of the mean correction factor b and the predicted resistance $r_{t,i}$ [47], and $r_{n,i}$ is the resistance predicted using the proposed design method with nominal material properties. The nominal material properties are calculated based on the material overstrength factors MF, which represent the ratio of mean to nominal yield strength $f_{y,mean}/f_{y,nom}$, as specified in [56] and listed in Table 6.

The key reliability analysis results for all considered cases are reported in Table 6. It can be observed that the b values are greater than 1 for all material grades, indicating that the mean predictions obtained through the design proposals are safe-sided. According to EN 1993–1–4:2025 [15], the partial safety factor for the stability design of stainless steel members γ_{M1} is taken as 1.1. The calculated required partial safety factor values $\gamma_{M1}{}^{*}$ are almost identical to the target value $\gamma_{M1} = 1.1$ for austenitic and ferritic stainless steel members, but slightly higher than the target value $\gamma_{M1} = 1.1$ for duplex stainless steel members. However, in line with the recommendations given in SAFEBRICTILE [59,60], an acceptance limit f_a is defined to allow a small exceedance of the target safety factor due to the influence of the combined variability of the resistance model and the basic variables, as given by:

$$f_a = 1.03 + 0.75(V_r - 0.04) \quad \text{but } 1.03 \le f_a \le 1.15 \tag{27}$$

V_r in Eq. (27) is the combined coefficient of variation incorporating the variability of the resistance model and the basic variables, as expressed by:

$$V_r = \sqrt{V_{rt}{}^2 + V_\delta{}^2} \tag{28}$$

where V_δ is the coefficient of variation of the benchmark FE results relative to the predicted resistances. Note that the V_r values vary for each case due to the variation in V_{rt}; thus, the V_r values provided in Table 6 correspond to the mean values.

As can be seen from Table 6, for all stainless steel grades the reliability requirement of $\gamma_{M1}{}^{*}/\gamma_{M1} \le f_a$ is satisfied. This indicates that the proposed design method is suitable for use in the stability design of laterally unrestrained stainless steel beam-columns in conjunction with the partial safety factor $\gamma_{M1} = 1.1$, as recommended in EN 1993–1–4:2025 [15].

5. Conclusions

In this study, new design rules have been developed for laterally unrestrained stainless steel I-section beam-columns under combined compression and uniform or non-uniform bending moments. A comprehensive parametric study using shell FE models was conducted to generate benchmark member resistances and investigate member behaviour. In total, 3250 beam-columns were evaluated, considering austenitic, duplex and ferritic stainless steel grades, as well as various cross-section geometries (Class 1–3), member slendernesses and interaction levels of applied axial compression and major axis bending. Calibrated against the benchmark FE results, interaction factors k_{zy} for the out-of-plane buckling check in the design of stainless steel beam-columns were proposed. The new proposals have been thoroughly assessed and shown to provide accurate, safe and consistent member resistance predictions. A reliability analysis of the proposed design rules

Table 6
Summary of reliability analysis for the proposed interaction factors against the benchmark shell FE results for all studied members.

Grade	n	b	V_{fy}	MF	V_δ	V_r	$\gamma_{M1}{}^{*}$	$\gamma_{M1}{}^{*}/\gamma_{M1}$	f_a
Austenitic	1136	1.097	0.11	1.25	0.059	0.10	1.105	1.004	1.076
Duplex	975	1.117	0.07	1.10	0.082	0.10	1.176	1.070	1.076
Ferritic	1139	1.131	0.07	1.15	0.072	0.09	1.102	1.002	1.070

was also performed, with results indicating that the proposed design rules can be applied with the partial safety factor γ_{M1} of 1.1, as specified in EN 1993–1–4:2025 [15]. The proposed interaction factor formulation k_{zy} for stainless steel design mirrors the format included in EN 1993–1–1:2022 [13] for carbon steel design, and the proposals have been included in the new version of the European structural stainless steel design standard EN 1993–1–4:2025 [15]. Future research will focus on the behaviour of laterally restrained stainless steel beam-columns and cross-section interaction between compression and bending.

CRediT authorship contribution statement

Chunyan Quan: Writing – original draft, Visualization, Software, Methodology, Investigation, Formal analysis, Data curation, Conceptualization. **Fiona Walport:** Writing – review & editing, Writing – original draft, Visualization, Methodology, Investigation, Formal analysis, Conceptualization. **Merih Kucukler:** Writing – review & editing, Visualization, Supervision, Methodology, Investigation, Formal analysis, Conceptualization. **Leroy Gardner:** Writing – review & editing, Visualization, Supervision, Project administration, Methodology, Investigation, Formal analysis, Conceptualization.

Declaration of Competing Interest

The authors declare that there is no conflict of interest.

Data availability

Data will be made available on request.

References

[1] Gardner L. Stability and design of stainless steel structures–Review and outlook. Thin Walled Struct 2019;141:208–16.
[2] Zhao O, Rossi B, Gardner L, Young B. Experimental and numerical studies of ferritic stainless steel cross-sections under combined compression and bending. J Struct Eng ASCE 2016;142(2):04015110.
[3] Zhao O, Rossi B, Gardner L, Young B. Behaviour of structural stainless steel cross-sections under combined loading – Part II: numerical modelling and design approach. Eng Struct 2015;89:247–59.
[4] Yuan HX, Wang YQ, Gardner L, Shi YJ. Local-overall interactive buckling of welded stainless steel box section compression members. Eng Struct 2014;67:62–76.
[5] Zhao O, Gardner L, Young B. Buckling of ferritic stainless steel members under combined axial compression and bending. J Constr Steel Res 2016;117:35–48.
[6] Gardner L, Bu Y, Theofanous M. Laser-welded stainless steel I-sections: Residual stress measurements and column buckling tests. Eng Struct 2016;127:536–48.
[7] Bu Y, Gardner L. Finite element modelling and design of welded stainless steel I-section columns. J Constr Steel Res 2019;152:57–67.
[8] Bu Y, Gardner L. Local stability of laser-welded stainless steel I-sections in bending. J Constr Steel Res 2018;148:49–64.
[9] Fortan M, Rossi B. Lateral torsional buckling of welded stainless steel I-profile beams: experimental study. ASCE J Struct Eng 2021;147:04020342.
[10] Fortan M, Rossi B. Lateral Torsional Buckling of Welded Stainless-Steel I-Profile Beams: Design and Reliability. ASCE J Struct Eng 2020;146:04020280.
[11] Zhao O, Gardner L, Young B. Behaviour and design of stainless steel SHS and RHS beam-columns. Thin Walled Struct 2016;106:330–45.
[12] Bu Y, Gardner L. Laser-welded stainless steel I-section beam-columns: testing, simulation and design. Eng Struct 2019;179:23–36.
[13] EN 1993-1-1:2022. Eurocode 3: Design of steel structures - Part 1-1: General rules and rules for buildings. Brussels: European Committee for Standardization; 2022.
[14] EN 1993-1-4:2006 + A1: 2015. Eurocode 3 - Design of steel structures - Part 1-4: General rules - Supplementary rules for stainless steels. Brussels: European Committee for Standardization; 2015.
[15] EN 1993-1-4:2025. Eurocode 3: Design of steel structures - Part 1-4: Stainless steel structures. Brussels: European Committee for Standardization; 2025.
[16] Kucukler M, Gardner L. In-plane structural response and design of duplex and ferritic stainless steel welded I-section beam–columns. Eng Struct 2021;247:113136.
[17] Greiner R, Lindner J. Interaction formulae for members subjected to bending and axial compression in Eurocode 3–The Method 2 approach. J Constr Steel Res 2006;62(8):757–70.
[18] Boissonnade N, Greiner R, Jaspart JP, Lindner J. Rules for Member Stability in EN 1993-1-1: Background Documentation and Design Guidelines, Publication No. 119. European Convention for Constructional Steelwork (ECCS); 2006.
[19] Kucukler M, Gardner L, Bu Y. Flexural-torsional buckling of austenitic stainless steel I-section beam-columns: Testing, numerical modelling and design. Thin Walled Struct 2020;152:106572.
[20] Taras A, Greiner R. New design curves for lateral-torsional buckling-Proposal based on a consistent derivation. J Constr Steel Res 2010;66:648–63.
[21] Knobloch M, Bureau A, Kuhlmann U, Simões da Silva L, Snijder HH, Taras A, Bours A-L, Jörg F. Structural member stability verification in the new Part 1-1 of the second generation of Eurocode 3: Part 2: Member buckling design rules and further innovations, Steel. Construction 2020;13:208–22.
[22] Taras A. Contribution to the development of consistent stability design rules for steel members (PhD thesis). Graz University of Technology; 2010.
[23] ABAQUS, SIMULIA-Dassault Systémes: Analysis User's Guide, Dassault Systémes Simulia Corp., Providence, USA, USA, 2021.
[24] Saliba N, Gardner L. Experimental study of the shear response of lean duplex stainless steel plate girders. Eng Struct 2013;46:375–91.
[25] Theofanous M, Chan TM, Gardner L. Flexural behaviour of stainless steel oval hollow sections. ThinWalled Struct 2009;47:776–87.
[26] Wang F, Young B, Gardner L. Experimental study of square and rectangular CFDST sections with stainless steel outer tubes under axial compression. J Struct Eng ASCE 2019;145:04019139.
[27] Kucukler M, Gardner L, Macorini L. Lateral-torsional buckling assessment of steel beams through a stiffness reduction method. J Constr Steel Res 2015;109:87–100.
[28] Quan C, Kucukler M, Gardner L. Design of web-tapered steel I-section members by second-order inelastic analysis with strain limits. Eng Struct 2020;224:111242.
[29] Quan C, Kucukler M, Gardner L. Out-of-plane stability design of steel beams by second-order inelastic analysis with strain limits. Thin Walled Struct 2021;169:108352.
[30] Valeš J, Stan TC. FEM Modelling of Lateral-Torsional Buckling Using Shell and Solid Elements. Procedia Eng 2017;190:464–71.
[31] Kucukler M. Stainless steel I-section beams at elevated temperatures: Lateral–torsional buckling behaviour and design. Thin Walled Struct 2025;208:112720.
[32] Arrayago I, Real E, Gardner L. Description of stress-strain curves for stainless steel alloys. Mater Des 2015;87:540–52.
[33] Afshan S, Zhao O, Gardner L. Standardised material properties for numerical parametric studies of stainless steel structures and buckling curves for tubular columns. J Constr Steel Res 2019;152:2–11.
[34] Osofero AI, Wadee MA, Gardner L. Experimental study of critical and post-buckling behaviour of prestressed stayed columns. J Constr Steel Res 2012;79:226–41.
[35] Fieber A, Gardner L, Macorini L. Formulae for determining elastic local buckling half-wavelengths of structural steel cross-sections. J Constr Steel Res 2019;159:493–506.
[36] EN 1090-2, EN 1090-2 - Execution of steel structures and aluminium structures. Part 2: Technical requirements for steel structures., BSI, 20182018.
[37] EN 1993-1-5:2024. Eurocode 3 - Design of steel structures - Part 1-5: Plated structural elements. Brussels: European Committee for Standardization; 2024.
[38] EN 1993-1-14:2025. Eurocode 3: Design of steel structures – Part 1-14: Design assisted by finite element analysis. Brussels: European Committee for Standardization; 2025.
[39] Lopes N, Couto C, Vila Real P, Camotim D, Gonçalves R. Fire design of stainless steel I beams prone to lateral torsional buckling under end moments. Fire Saf J 2022;131:103609.
[40] Yuan HX, Wang YQ, Shi YJ, Gardner L. Residual stress distributions in welded stainless steel sections. Thin Walled Struct 2014;79:38–51.
[41] Kucukler M, Xing Z, Gardner L. Behaviour and design of stainless steel I-section columns in fire. J Constr Steel Res 2020;164:105890.
[42] Jönsson J, Stan TC. European column buckling curves and finite element modelling including high strength steels. J Constr Steel Res 2017;128:136–51.
[43] Kala Z, Valeš J. Sensitivity assessment and lateral-torsional buckling design of I-beams using solid finite elements. J Constr Steel Res 2017;139:110–22.
[44] Walport F. Design of steel and stainless steel structures by advanced inelastic analysis (PhD thesis). Imperial College London; 2019.
[45] Theofanous M, Gardner L. Testing and numerical modelling of lean duplex stainless steel hollow section columns. Eng Struct 2009;31:3047–58.
[46] Schaper L, Jörg F, Winkler R, Kuhlmann U, Knobloch M. The simplified method of the equivalent compression flange: Development based on LTB tests and residual stress measurements. Steel Constr 2019;12:264–77.
[47] EN 1990:2023. Eurocode - Basis of structural and geotechnical design. Brussels, Belgium: CEN (European Committee for Standardization); 2023.
[48] Tankova T, Simões Da Silva L, Marques L, Rebelo C, Taras A. Towards a standardized procedure for the safety assessment of stability design rules. J Constr Steel Res 2014;103:290–302.
[49] Ditlevsen O, Madsen HO. Structural Reliability Methods. Chichester: John Wiley & Sons; 2005.
[50] T. Vrouwenvelder, S. Dimova, M.L. Sousa, J. Marková, G. Mancini, U. Kuhlmann, A. Taras, R. Jockwer, T. Jäger, W. Jäger, T. Schweckendiek, P. Franchin, D. Skejić, J.D. Sørensen, P. Spehl, Stacy, Reliability background of the Eurocodes, 2024.
[51] Bock M, Real E. Effective width equations accounting for element interaction for cold-formed stainless steel square and rectangular hollow sections. Structures 2015;2:81–90.
[52] Jönsson J, Müller MS, Gamst C, Valeš J, Kala Z. Investigation of European flexural and lateral torsional buckling interaction. J Constr Steel Res 2019;156:105–21.
[53] Afshan S, Francis P, Baddoo NR, Gardner L. Reliability analysis of structural stainless steel design provisions. J Constr Steel Res 2015;114:293–304.
[54] Walport F, Gardner L, Nethercot DA. Equivalent bow imperfections for use in design by second order inelastic analysis. Structures 2020;26:670–85.

[55] Walport F, Gardner L, Nethercot DA. Design of structural stainless steel members by second order inelastic analysis with CSM strain limits. ThinWalled Struct 2020; 159:107267.
[56] Meza FJ, Baddoo N, Gardner L. Derivation of stainless steel material factors for European and U.S. design standards. J Constr Steel Res 2024;213:108383.
[57] Meng X, Gardner L. Behavior and design of normal- and high-strength steel SHS and RHS columns. ASCE J Struct Eng 2020;146:04020227.
[58] Quan C, Walport F, Gardner L. Equivalent geometric imperfections for the design of steel and stainless steel beam-columns by GMNIA. J Constr Steel Res 2024;215: 108502.
[59] SAFEBRICTILE. 2016. Standardization of safety assessment procedures across brittle to ductile failure modes. Grant Agreement Number: RFSR-CT-2013-00023, Deliverable D1.1 - Guideline for the Safety Assessment of Design Rules for Steel Structures in Line with EN 1990.
[60] HOLLOSSTAB. 2019. Overall-slenderness based direct design for strength and stability of innovative hollow sections. Grant Agreement Number: RFCS-2015-709892, Deliverable D7.2 - Reliability Analysis of the Design Proposals and Determination of Partial Factors.